Supplement of Biogeosciences, 21, 2313–2333, 2024
https://doi.org/10.5194/bg-21-2313-2024-supplement

Biogeosciences
Open Access

Supplement of

Modeling microbial carbon fluxes and stocks in global soils from 1901 to 2016

Liyuan He et al.

Correspondence to: Xiaofeng Xu (xxu@sdsu.edu)

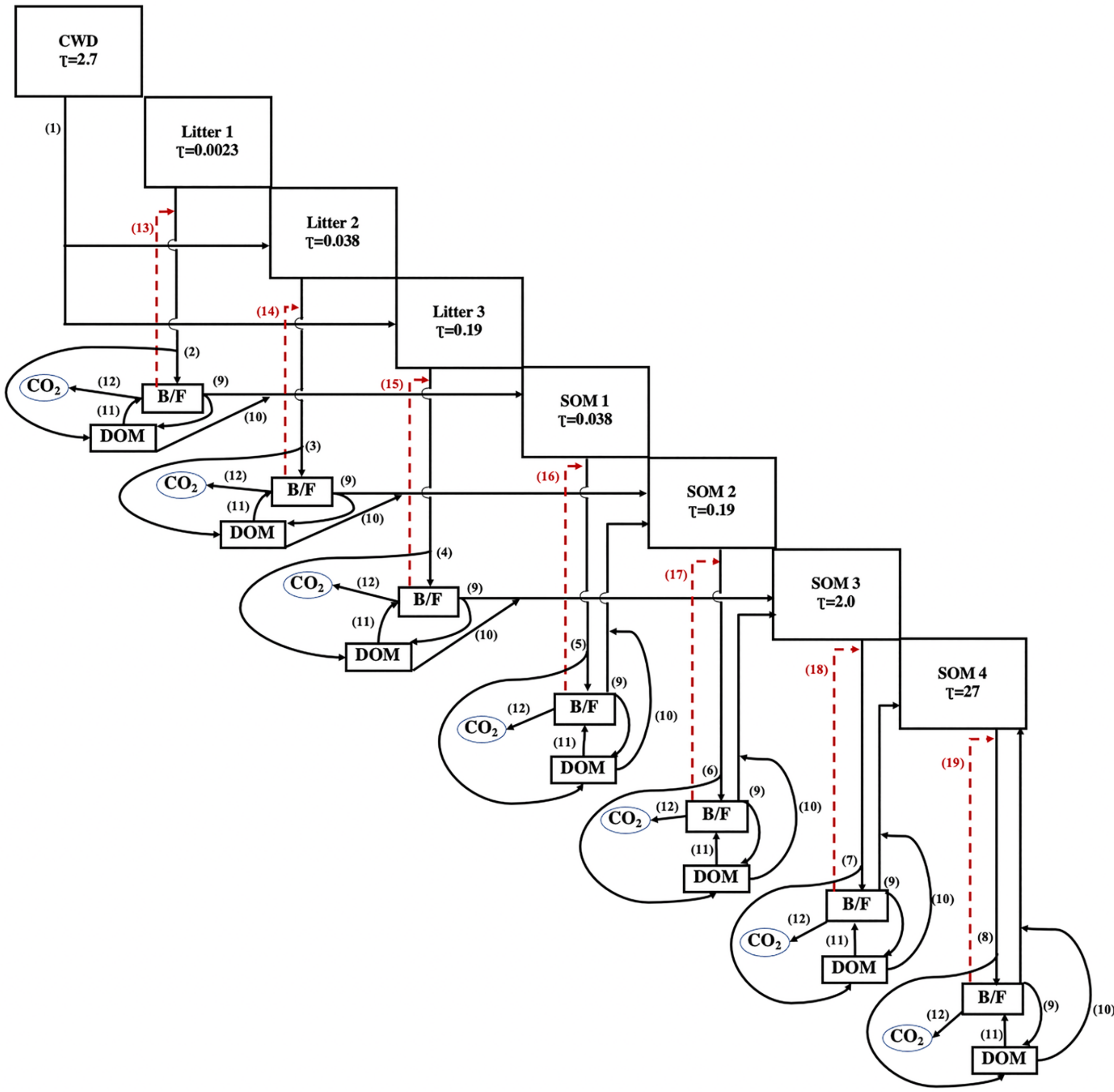

Fig. S1. Conceptual diagram showing the key processes and the roles of fungi and bacteria in the CLM-Microbe model. CWD, coarse woody debris; SOM, soil organic matter; B, bacteria; F, fungi; DOM, dissolved organic matter. In the CLM-Microbe model, number in the box means turnover time of each pool. Black solid lines indicate transitions in the CLM-Microbe model, which generally represents processes such as 1) decomposition of coarse woody debris, 2) litter 1 decomposition, 3) litter 2 decomposition, 4) litter 3 decomposition, 5) soil organic matter 1 decomposition, 6) soil organic matter 2 decomposition, 7) soil organic matter 3 decomposition, 8) soil organic matter 4 decomposition, 9) fungal and bacterial lysis, 10) dissolved organic matter adsorption, 11) dissolved organic matter uptake by fungal and bacterial, and 12) fungal and bacterial respiration. Red dash lines represent regulatory role of fungi and bacteria on the process, including fungi and bacteria regulation on 13) litter 1, 14) litter 2, 15) litter 3, 16) soil organic matter 1, 17) soil organic matter 2, 18) soil organic matter 3, and 19) soil organic matter 4 decomposition (He et al., 2021).

Table S1. Key model parameters in processes involving fungal and bacterial biomass

Symbol	Range [a]	Unit	Description	Reference
k_dom	0.0025-0.5	d^{-1}	decomposition rate constant of DOM	(Wheeler et al., 1996; Kirchman et al., 1991; Cherrier et al., 1996)
k_bacteria	0.00143-2	d^{-1}	lysis rate constant of bacteria	(Rousk and Bååth, 2007, 2011; Moore et al., 2005; Schippers et al., 2005)
k_fungi	0.00027-0.05	d^{-1}	lysis rate constant of fungi	(Thornton and Rosenbloom, 2005; Rousk and Bååth, 2011; Moore et al., 2005; Wallander et al., 2004)
m_rf_s1m	0-1		fraction factor quantifying carbon from SOM1 to microbes	Calibrated
m_rf_s2m	0-1		fraction factor quantifying carbon from SOM2 to microbes	Calibrated
m_rf_s3m	0-1		fraction factor quantifying carbon from SOM3 to microbes	Calibrated
m_rf_s4m	0-1		fraction factor quantifying carbon from SOM4 to microbes	Calibrated
m_batm_f	0-1		fraction factor quantifying carbon respired by bacteria	Calibrated
m_bdom_f	0-1		fraction factor quantifying carbon from DOM to bacteria	Calibrated
m_bs1_f	0-1		fraction factor quantifying carbon from bacteria to SOM1	Calibrated
m_bs2_f	0-1		fraction factor quantifying carbon from bacteria to SOM2	Calibrated
m_bs3_f	0-1		fraction factor quantifying carbon from bacteria to SOM3	Calibrated
m_fatm_f	0-1		fraction factor quantifying carbon respired by fungi	Calibrated
m_fdom_f	0-1		fraction factor quantifying carbon from DOM to fungi	Calibrated
m_fs1_f	0-1		fraction factor quantifying carbon from fungi to SOM1	Calibrated
m_fs2_f	0-1		fraction factor quantifying carbon from fungi to SOM2	Calibrated
m_fs3_f	0-1		fraction factor quantifying carbon from fungi to SOM3	Calibrated
m_domb_f	0-1		fraction factor quantifying carbon from DOM to bacteria	Calibrated
m_domf_f	0-1		fraction factor quantifying carbon from DOM to fungi	Calibrated
m_doms1_f	0-1		fraction factor quantifying carbon from DOM to SOM1	Calibrated
m_doms2_f	0-1		fraction factor quantifying carbon from DOM to SOM2	Calibrated
m_doms3_f	0-1		fraction factor quantifying carbon from DOM to SOM3	Calibrated
cn_bacteria	3-12		C:N ratio of bacteria	(Strickland and Rousk, 2010)
cn_fungi	3-60		C:N ratio of fungi	(Strickland and Rousk, 2010)
cn_dom	4.2-185		C:N ratio of DOM	(Sinsabaugh et al., 2016)
CUEmax	0.46-0.9		maximum carbon use efficiency of microbes	(Gommers et al., 1988; Sinsabaugh et al., 2013; Sinsabaugh et al., 2016)

[a]The values may not be the same as those from literature sources due to unit conversion.

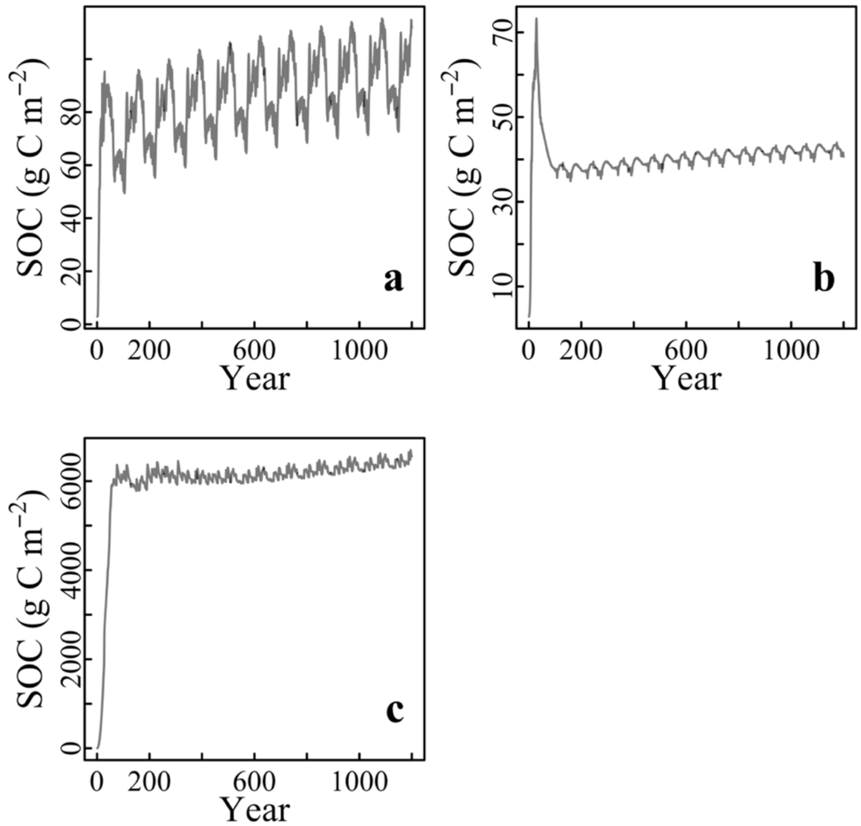

Fig. S2 Evolution of total soil organic carbon density at the a) low-latitude (0.98°N, 42.5°E), b) low-latitude (36.9°N, 42.5°E), and c) high-latitude (67.3°N, 42.5°E) grid cells from cold start simulated by the CLM-Microbe model.

Table S2. Site information of the observational data of dissolved organic carbon in the top 30 cm

ID	Biome	Latitude	Longitude	Country	Reference
01	Boreal forest	43.926	-71.676	USA	Mcdowell and Wood (1984)
02	Boreal forest	51.3	4.517	Belgium	Camino-Serrano et al. (2018)
03	Boreal forest	58.133	-3.883	UK	Cookson et al. (2007)
04	Grassland	23.91	120.559	China	Liu et al. (2009)
05	Grassland	31.717	121.5	China	Wang et al. (2015)
06	Grassland	35	139	Japan	Kawahigashi et al. (2003)
07	Grassland	50.783	10.217	Germany	Don and Schulze (2008)
08	Grassland	58.133	-3.883	UK	Cookson et al. (2007)
09	Natural wetland	30.754	120.759	China	Shao et al. (2015)
10	Natural wetland	36.117	120.1	China	Xi et al. (2018)
11	Natural wetland	36.217	120.1	China	Xi et al. (2018)
12	Natural wetland	46.43	11.412	Italy	Zeh et al. (2019)
13	Natural wetland	46.478	11.075	Italy	Zeh et al. (2019)
14	Paddy	14.625	120.375	Philippines	Lu et al. (2000)
15	Paddy	28	116	China	Wu et al. (2019)
16	Paddy	30.479	114.353	China	Liu et al. (2014)
17	Shrubland	23.91	120.559	China	Liu et al. (2009)
18	Shrubland	28.092	116.092	China	Yao et al. (2009)
19	Shrubland	31.717	121.5	China	Wang et al. (2015)
20	Temperate broadleaf forest	22.892	113.803	China	Zhong et al. (2017)
21	Temperate broadleaf forest	28.092	116.092	China	Yao et al. (2009)
22	Temperate broadleaf forest	29.3333	115.9333	China	Li et al. (2013)
23	Temperate broadleaf forest	35	139	Japan	Kawahigashi et al. (2003)
24	Temperate broadleaf forest	48.417	14.061	Germany	Maxin and Kögel-Knabner (1995)
25	Temperate broadleaf forest	51.067	10.45	Germany	Camino-Serrano et al. (2018)
26	Temperate broadleaf forest	56.083	12.733	Ecuador	Andreasson et al. (2009)
27	Temperate broadleaf forest	56.117	12.617	Ecuador	Andreasson et al. (2009)
28	Temperate needleleaf forest	-38	175	New Zealand	Ghani et al. (2007)
29	Temperate needleleaf forest	26.747	115.07	China	Ying et al. (2013)
30	Temperate needleleaf forest	44.2314	-122.2278	USA	Spears et al. (2003)
31	Temperate needleleaf forest	53.1	-4.15	UK	Jones et al. (2008)
32	Tropical dry forest	-2.609	-60.209	Brazil	Marques et al. (2012)
33	Tropical dry forest	19.483	-104.517	Mexico	Montano et al. (2009)
34	Tropical dry forest	23	121	China	Liu and Sheu (2003)
35	Tropical dry forest	23.17	112.57	China	Fang et al. (2014a)
36	Tropical dry forest	29.3333	115.9333	China	Li et al. (2013)
37	Tropical rain forest	-2.533	-60.033	Brazil	Marques et al. (2012)
38	Tropical rain forest	-1.85	116.0333	Indonesia	Fujii et al. (2011)
39	Tropical rain forest	-1.8167	115.9833	Indonesia	Fujii et al. (2011)
40	Tropical rain forest	-1.0167	116.8667	Indonesia	Fujii et al. (2009)
41	Tropical rain forest	-0.85	117.1	Indonesia	Fujii et al. (2009)
42	Tropical rain forest	10.4333	-83.9833	Costa Rica	Schwendenmann and Veldkamp (2005)
43	Tropical rain forest	21.933	101.25	China	Zhou et al. (2016)
44	Tundra	29.3333	115.9333	China	Li et al. (2013)
45	Tundra	37.6167	-101.3167	China	Fang et al. (2014b)
46	Tundra	64.867	-149.066	USA	Neff and Hooper (2002)
47	Tundra	64.867	-147.783	USA	Neff and Hooper (2002)
48	Tundra	67.65	-149.716	USA	Neff and Hooper (2002)
49	Tundra	68.6333	-149.6333	USA	Weintraub and Schimel (2005)

Table S3. Site information of the observational data of dissolved organic carbon in the top 1 m

ID	Biome	Latitude	Longitude	Country	Reference
01	Boreal forest	-2.8	-79.15	Ecuador	Pesántez et al. (2018)
02	Boreal forest	-2.783	-79.233	Ecuador	Pesántez et al. (2018)
03	Boreal forest	64.233	19.767	Ecuador	Panneer Selvam et al. (2016)
04	Boreal forest	64.8687	-147.8604	USA	Waldrop et al. (2010)
05	Grassland	-2.783	-79.233	Ecuador	Pesántez et al. (2018)
06	Grassland	23.91	120.559	China	Liu et al. (2009)
07	Grassland	31.717	121.5	China	Wang et al. (2015).
08	Grassland	35	139	Japan	Kawahigashi et al. (2003)
09	Grassland	35.35	139.467	Japan	Kawahigashi et al. (2003)
10	Grassland	50.783	10.217	Germany	Don and Schulze (2008)
11	Grassland	52.867	-6.9	Ireland	Camino-Serrano et al. (2018)
12	Grassland	64.183	19.55	Ecuador	Ågren et al. (2012)
13	Natural wetland	36.117	120.1	China	Xi et al. (2018)
14	Natural wetland	36.167	120.1	China	Xi et al. (2018)
15	Natural wetland	43.074	144.391	Japan	Senga et al. (2011)
16	Shrubland	23.91	120.559	China	Liu et al. (2009)
17	Shrubland	31.717	121.5	China	Wang et al. (2015)
18	Temperate broadleaf forest	-30.577	115.876	Australia	Macdonald et al. (2007)
19	Temperate broadleaf forest	31.717	121.5	China	Wang et al. (2015)
20	Temperate broadleaf forest	33.15	130.466	Japan	Funakawa et al. (1992)
21	Temperate broadleaf forest	35	139	Japan	Kawahigashi et al. (2003)
22	Temperate broadleaf forest	35.35	139.467	Japan	Kawahigashi et al. (2003)
23	Temperate broadleaf forest	35.967	-84.267	USA	Fröberg et al. (2007)
24	Temperate needleleaf forest	26.747	115.07	China	Ying et al. (2013)
25	Temperate needleleaf forest	44.2314	-122.2278	USA	Spears et al. (2003)
26	Tropical dry forest	-2.609	-60.209	Brazil	Marques et al. (2012)
27	Tropical rain forest	10.4333	-83.9833	Costa Rica	Schwendenmann and Veldkamp (2005)
28	Tropical rain forest	21.933	101.25	China	Zhou et al. (2016)

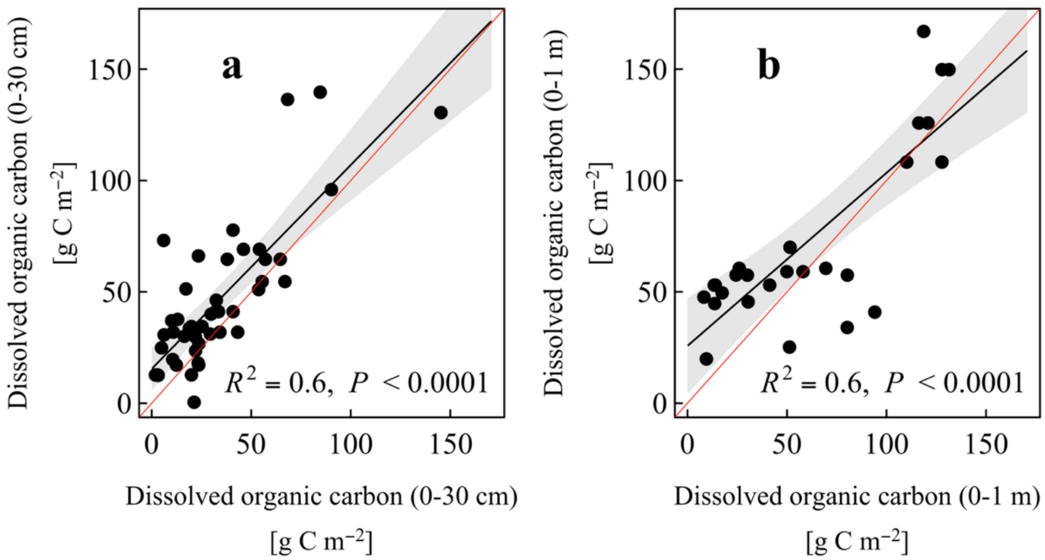

Fig. S3 Comparison of dissolved organic carbon in top 30 cm (a) and 1 m (b) between observed and simulated values.

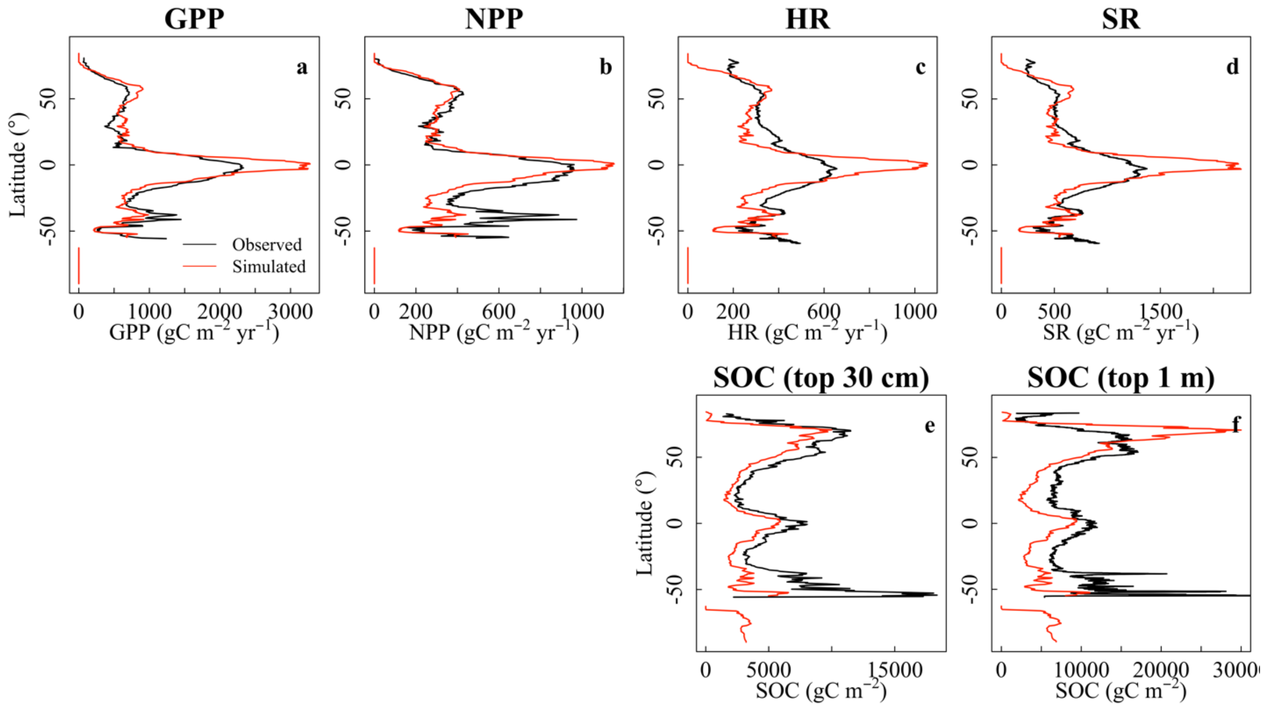

Fig. S4. Latitudinal comparison between observed (black line) and the CLM4.5-simulated (red line) latitudinal gradients of (a) GPP, (b) NPP, (c) HR, (d) SR, (e) SOC in the top 30 cm, and (f) SOC in the top 1 m. GPP: gross primary productivity; NPP: net primary productivity; HR: heterotrophic respiration; SR: soil respiration; SOC: soil organic carbon.

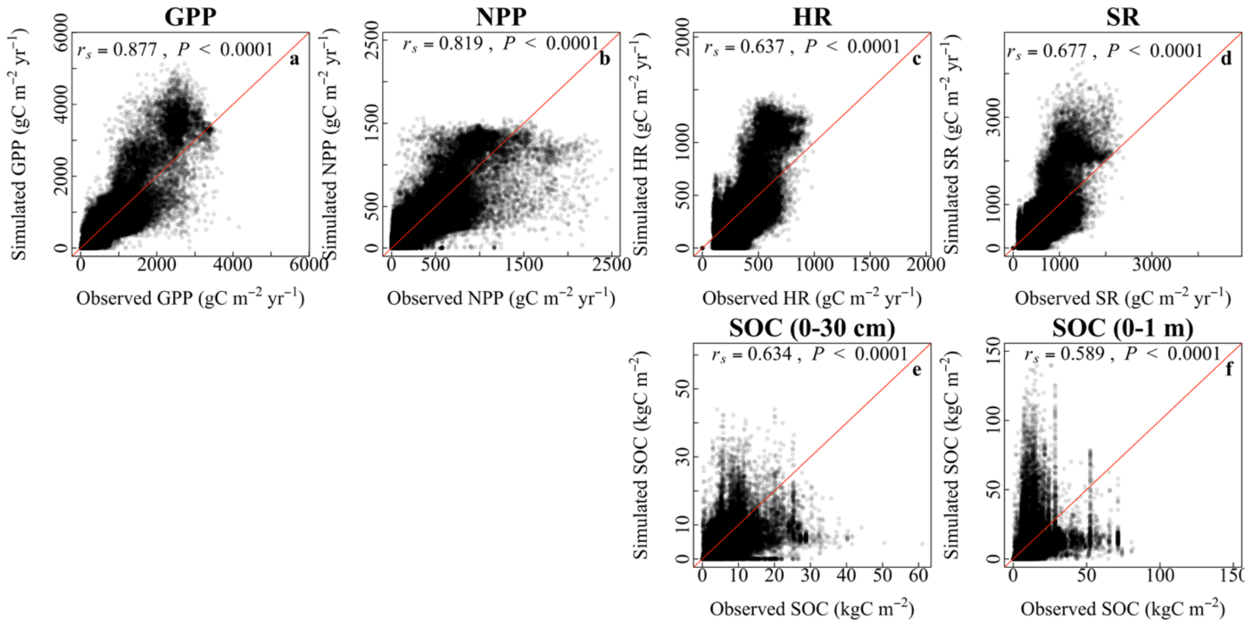

Fig. S5. Grid-by-grid comparison between observed and the CLM4.5-simulated grid cells of (a) GPP, (b) NPP, (c) HR, (d) SR, € SOC in the top 30 cm, and (f) SOC in the top 1 m. Red lines are 1:1 line. GPP: gross primary productivity; NPP: net primary productivity; HR: heterotrophic respiration; SR: soil respiration; SOC: soil organic carbon.

Table S4. Validation and atmospheric forcing datasets used in this study

Variables	Dataset	Source
Gross and net primary productivity	MODIS gridded datasets	Zhao et al. (2005)
Heterotrophic and soil respiration	Global Gridded 1-km Annual Soil Respiration Database	Warner et al. (2019)
Soil organic carbon (0-1 m)	Harmonized World Soil Database	Wieder (2014)
Soil organic carbon (0-30 cm)	Global Soil Organic Carbon Map	Fao (2018)
Fungal and bacterial biomass carbon (0-30 cm)	Global Topsoil Fungal and Bacterial Biomass Carbon Dataset	He et al. (2020)
Microbial biomass carbon (0-1 m)	Global Soil Microbial Biomass Carbon, Nitrogen, and Phosphorus Dataset	Xu et al. (2013)
Dissolved organic carbon (0-30 cm & 0-1 m)	Global Dissolved Organic Carbon Dataset	Guo et al. (2020)
Meteorological Forcing	CRUNCEP Version 7 - Atmospheric Forcing Data for the Community Land Model	Viovy (2018)

During 1901-2016, the decadal average of soil C was the largest C pool in the soil-vegetation-litter system, about 15 times of the sum of vegetation and litter C (Table 2). Soil, litter, and vegetation C significantly increased from 1901-1911 to 2007-2016 ($P<0.05$). However, the absolute increase in those C pools were different, with soil (37.0 PgC) and vegetation (37.1 PgC) increased to a larger extent than litter (5.1 PgC). Although soil and vegetation increased to a similar extent, vegetation (19.2%) showed a larger relative increase than soil (0.8%) due to its smaller pool size. Despite the smallest absolute increase, litter (8.0%) increased more than soil with respect to relative values.

Table S5. Carbon stock of vegetation, litter, and soil pools and absolute and relative changes from 1901-1910 to 2007-2016

	Total Carbon stock (PgC)		Change from 1901-1910 to 2007-2016	
Pool	1901-1910	2007-2016	Absolute change (PgC)	Relative change (%)
SOC	4527 (0.4)	4564 (1.8)	37.0*	0.8
Litter	63 (0.2)	68 (0.4)	5.1*	8.0
Vegetation	193 (1.1)	230 (2.9)	37.1*	19.2

Numbers in parentheses represent standard deviation. * indicates significant absolute change from 1901-1910 to 2007-2016 at $\alpha = 0.05$.

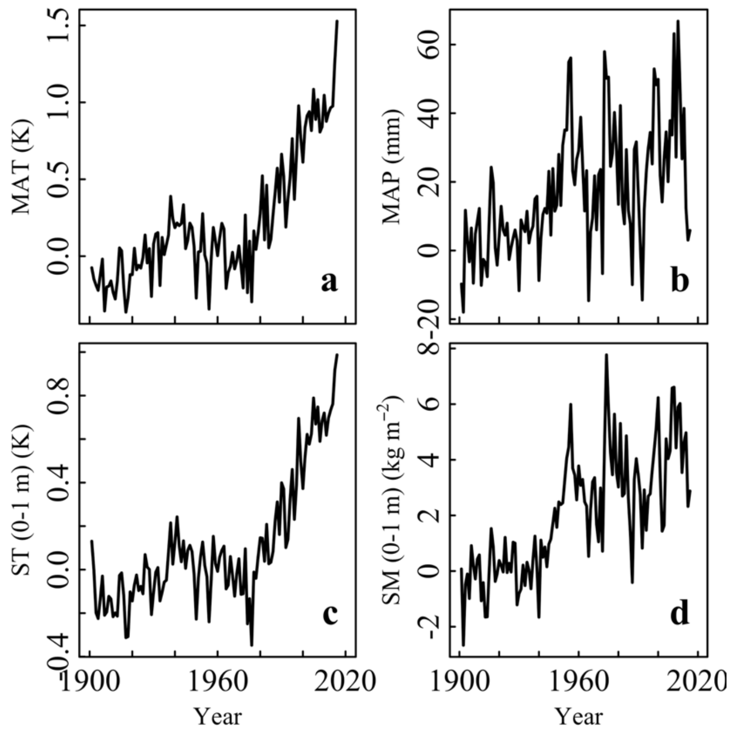

Fig. S6 Temporal variations of annual deviations in (a) MAT, (b) MAP, (c) ST of top 1m, and (d) SM of top 1m weighted by area in the CLM-Microbe model from 1901-1910. The baseline was the ten-year average of corresponding variables during 1901-1910. MAT, mean annual temperature; MAP, mean annual precipitation; ST, soil temperature; SM, soil moisture.

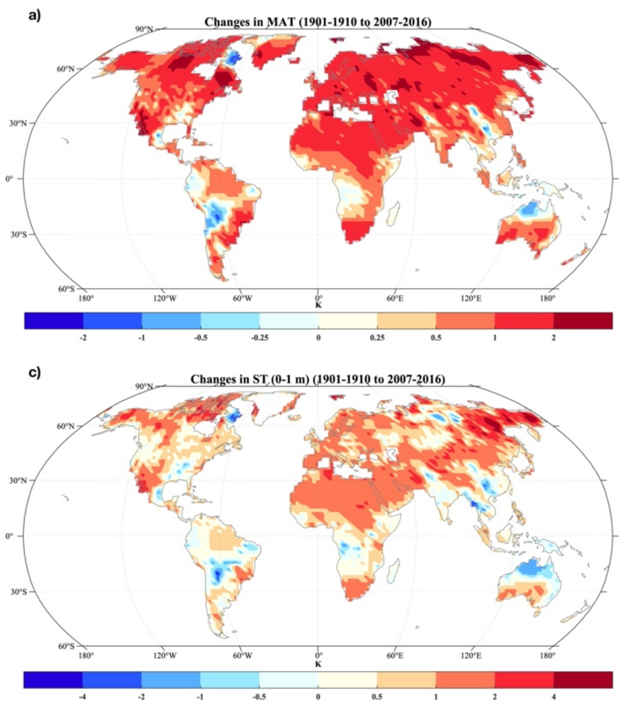

Fig. S7 Changes of (a) MAT, (b) MAP, (c) ST (0-1 m), and (d) SM (0-1 m) in 2007-2016 vs. 1901-1910. MAT, mean annual temperature; MAP, mean annual precipitation; ST, soil temperature; SM, soil moisture.

The GPP and NPP displayed increasing trends from 1901 to 2016 (Figure S8a & S8b), with different magnitudes among variables. By 2016, GPP (30 PgC yr^{-1}) increased about twice more than NPP (13 PgC yr^{-1}). Their increasing rates showed variations with time. We observed a relatively modest increase in GPP and NPP during 1901-1980, whereas their increases were more rapid from 1981 to 2016.

Vegetation, litter, and soil C pools increased from 1901 to 2016 despite the year-to-year variability (Figure S8c-S8f). The VegC and DOC, SOC, and LitC in the top 1 m increased by about 37, 2.4, 34, and 4 PgC, respectively, from 1901 to 2016. However, the temporal trends of those variables varied during 1901-2016 (Figure S8d-S8f). The VegC and LitC and SOC in the top 1 m showed a steady increase during 1901-2016, while DOC (0-1 m) slightly decreased from 1901 to 1920 but increased after 1920.

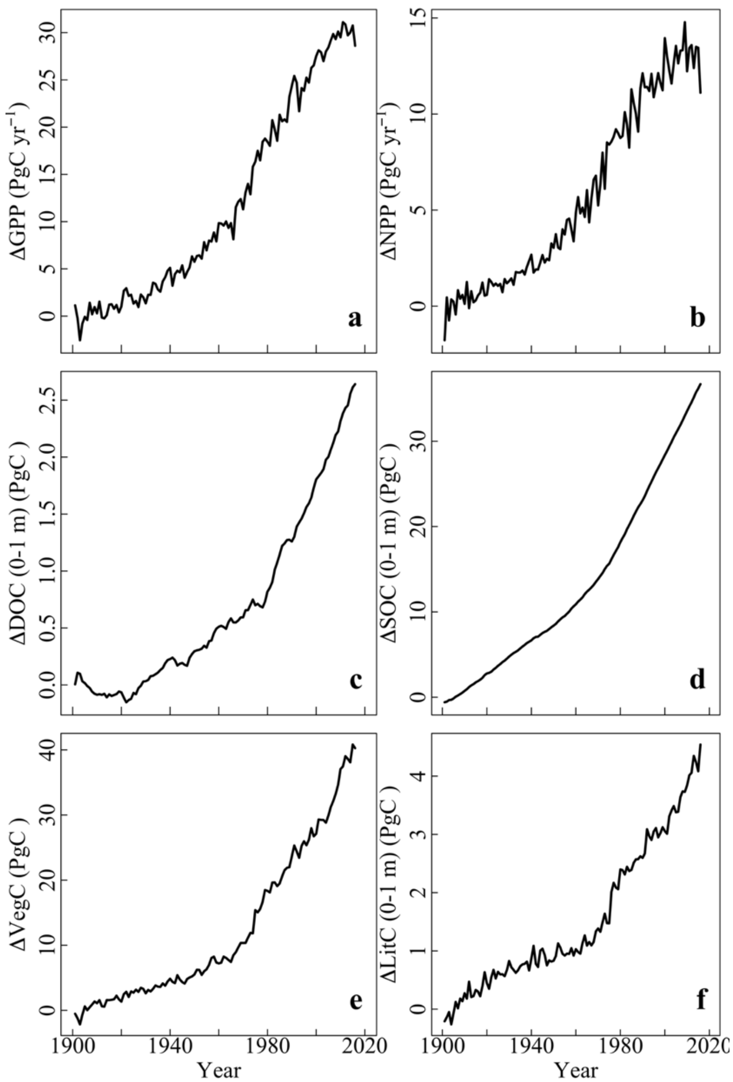

Fig. S8. Evolution of annual carbon flux of area-weighted (a) GPP and (b) NPP and annual carbon stock of (c) DOC in the top 1 m, (d) SOC in the top 1 m, (e) VegC, and (f) LitC in the top 1 m simulated by the CLM-Microbe model since 1901. The baseline was the ten-year average of corresponding variables during 1901-1910. GPP: gross primary productivity; NPP: net primary productivity; DOC: dissolved organic carbon; SOC: soil organic carbon; VegC: vegetation carbon; LitC: litter carbon.

Compared with 1901-1910, GPP and NPP increased across latitudinal gradients in 2007-2016 (Figure S9a-S9b). However, the magnitude of the increase differed among latitudinal gradients. Specifically, increases in GPP and NPP were larger and more prominent at northern latitudes and equatorial regions than at southern latitudes. Similar to C fluxes, C pools in vegetation, soil, and litter increased across latitudinal gradients from 1901-1910 to 2007-2016 (Figure S9c-S9f). Overall, DOC, SOC, and LitC in the top 1 m, and VegC showed a small but to different extents of increase across latitudinal gradients. Specifically, the increases were more prominent at northern high latitudes and equatorial regions than at other latitudes.

Across the globe, GPP and NPP showed similar spatial patterns (Figure S9a-S9b) and increases in most grids across the globe were statistically significant ($P<0.05$; Figure S10a, S10b, S10d, and S10e). Correspondingly, we observed positive relative change in most areas from 1901-1910 to 2007-2016 (Figure S10c and S10f). However, we also observed decreases in GPP and NPP in the grids of South Asia. The GPP and NPP displayed similar spatial patterns of changing rates (Figure S12a-S12b). We widely observed significant and positive changing rates of GPP and NPP from 1901 to 2016 ($P<0.05$). However, we also found significant negative changing rates of GPP and NPP in grids of South Asia ($P<0.05$). DOC (0-1 m) showed increases from 1901-1910 to 2007-2016 (Figure S11a & S11b), and the relative changes in DOC (0-1 m) were mostly positive (Figure S11c). We also widely observed increases in SOC (0-1 m) by 2007-2016 relative to 1901-1910 (Figure S11d & S 11e), which reached the significance level of 0.05 (Figure S11f). The relative increases were widely positive, while grids of South Asia displayed decreases in SOC (0-1 m). The VegC and LitC (0-1 m) exhibited similar spatial patterns and widely increased across the globe (Figure S11g-12l). The relative change in both VegC and LitC (0-1 m) were mostly positive across the globe, but the magnitudes were different. The relative change in VegC was to a larger extent than in LitC (0-1 m). Despite the widely increase, both VegC and LitC (0-1 m) decreased in South Asia. Consistent with the spatial patterns of absolute and relative changes, increasing temporal trends of such variables were widely observed across the globe. However, we also observed decreases of those variables in South Asia (Figure S12). In addition, we observed decreases of DOC, and SOC in the top 1 m in grids of central North America (Figures S11a-S11f and S12c-S12d).

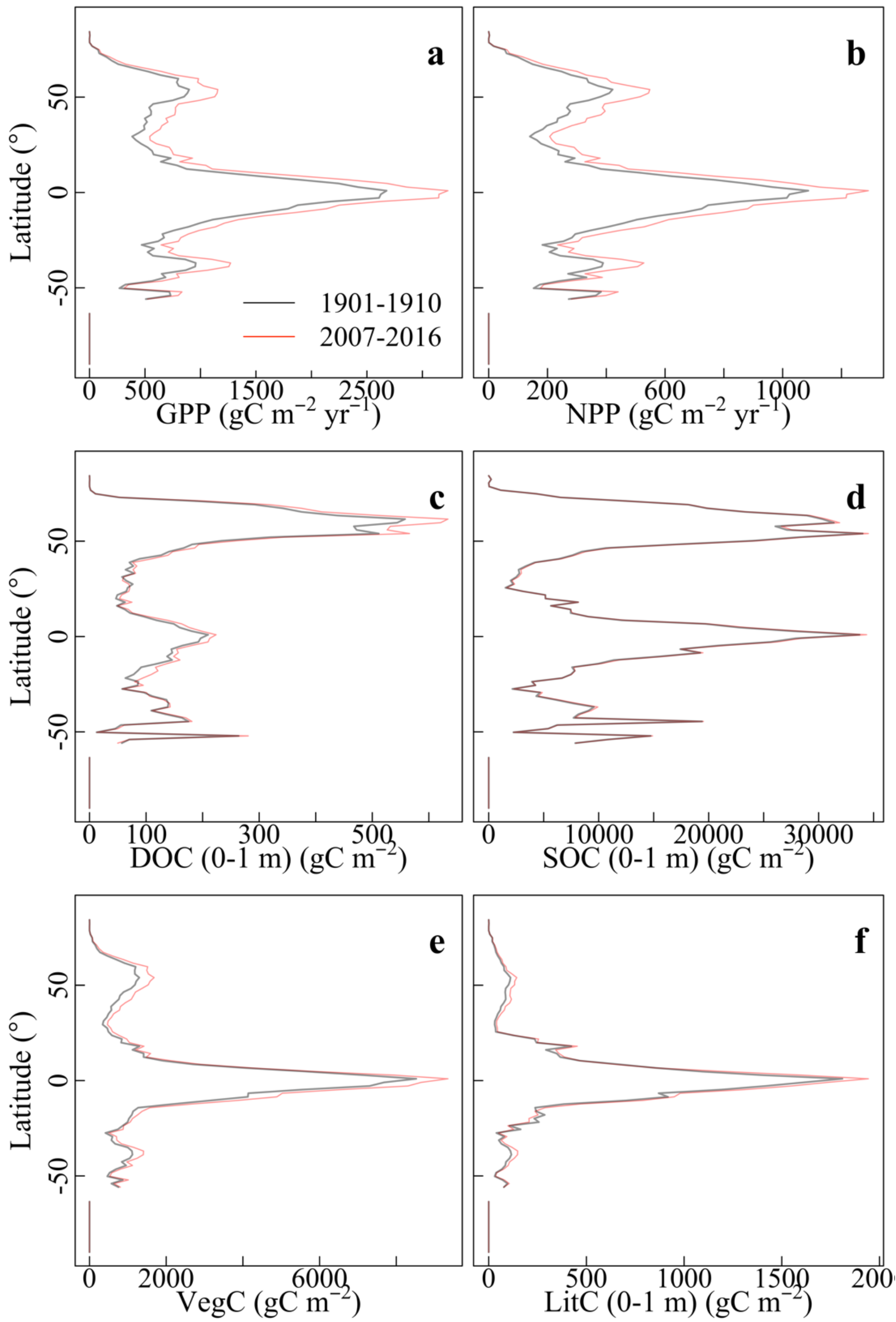

Fig. S9. Latitudinal gradients of the CLM-Microbe model simulated ten-year averages of (a) GPP and (b) NPP and annual carbon stock of (c) DOC in the top 1 m, (d) SOC in the top 1 m, (e) VegC, and (f) LitC in the top 1 m during 1901-1910 and 2007-2016. GPP: gross primary productivity; NPP: net primary productivity; DOC: dissolved organic carbon; SOC: soil organic carbon; VegC: vegetation carbon; LitC: litter carbon.

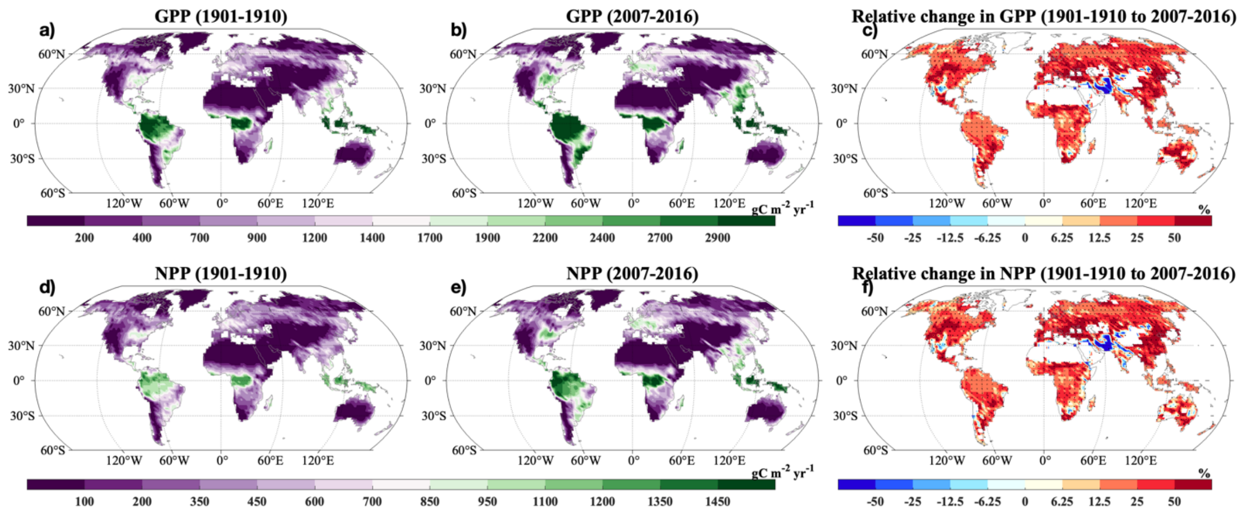

Fig. S10. Spatial distributions of decadal averages of (a-b) GPP and (d-e) NPP during (a and d) 1901-1910 and (b and e) 2007-2016 and relative changes in © GPP and (f) NPP by 2007-2016 relative to 1901-1910. GPP: gross primary productivity; NPP: net primary productivity. Black dot in each grid indicates significant changes (*P*<0.05).

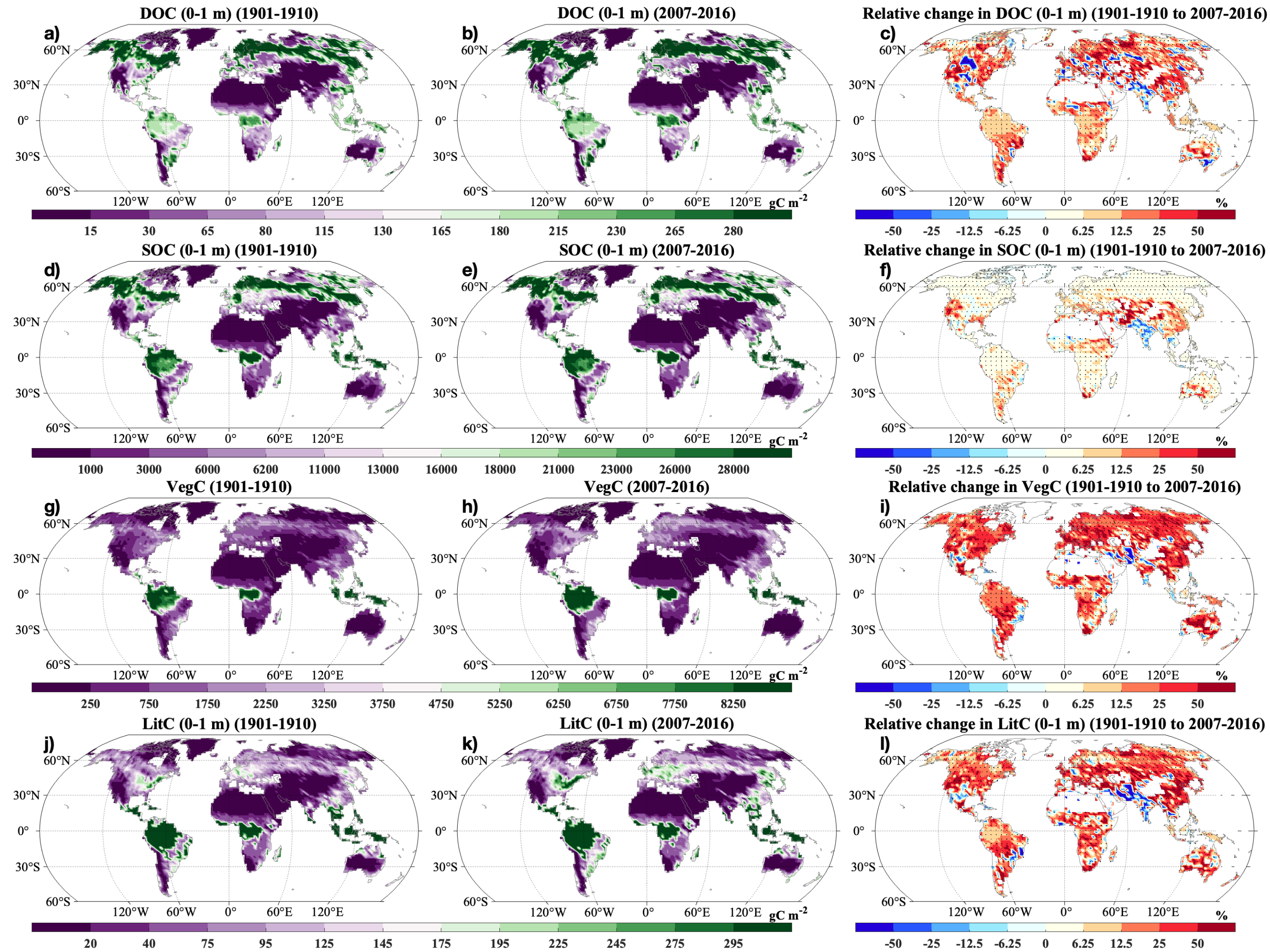

Fig. S11. Spatial distributions of decadal averages of (a-b) DOC in the top 1 m, (d-e) SOC in the top 1 m, (g-h) VegC, and (j-k) LitC in the top 1 m during (a, d, g, and j) 1901-1910 and (b, e, h, and k) 2007-2016 and relative changes in (c) DOC in the top 1 m, (f) SOC in the top 1 m, (i) VegC, and (l) LitC in the top 1 m by 2007-2016 relative to 1901-1910. DOC: dissolved organic carbon; SOC: soil organic carbon; VegC: vegetation carbon; LitC: litter carbon. Black dot in each grid indicates significant changes (P<0.05).

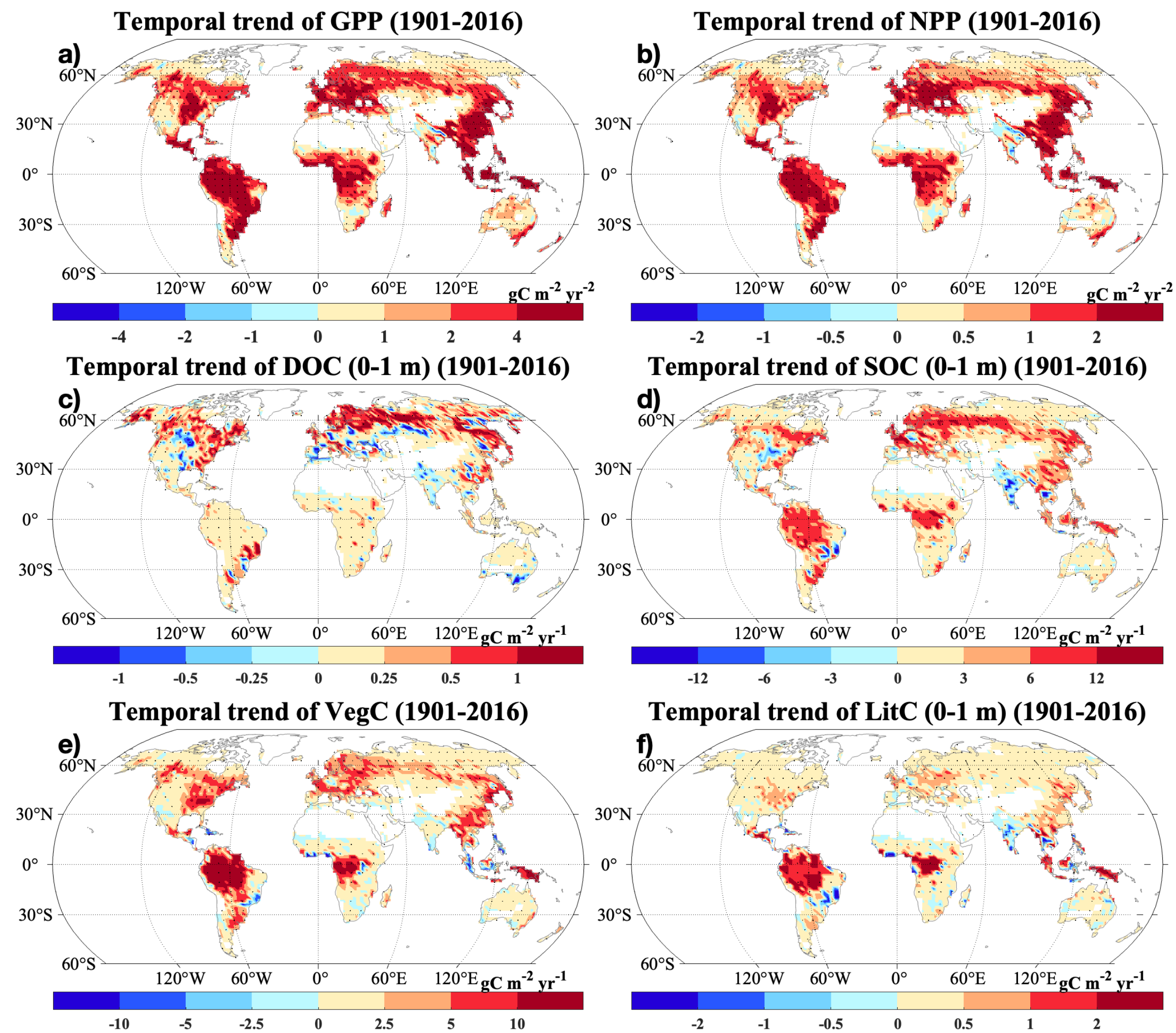

Fig. S12. Changing rates of the CLM-Microbe model simulated (a) GPP, (b) NPP, (c) DOC in the top 1 m, (d) SOC in the top 1 m, (e) VegC, and (f) LitC in the top 1 m from 1901 to 2016. GPP: gross primary productivity; NPP: net primary productivity; DOC: dissolved organic carbon; SOC: soil organic carbon; VegC: vegetation carbon; LitC: litter carbon. Black dot in each grid indicates significant regression (P<0.05).

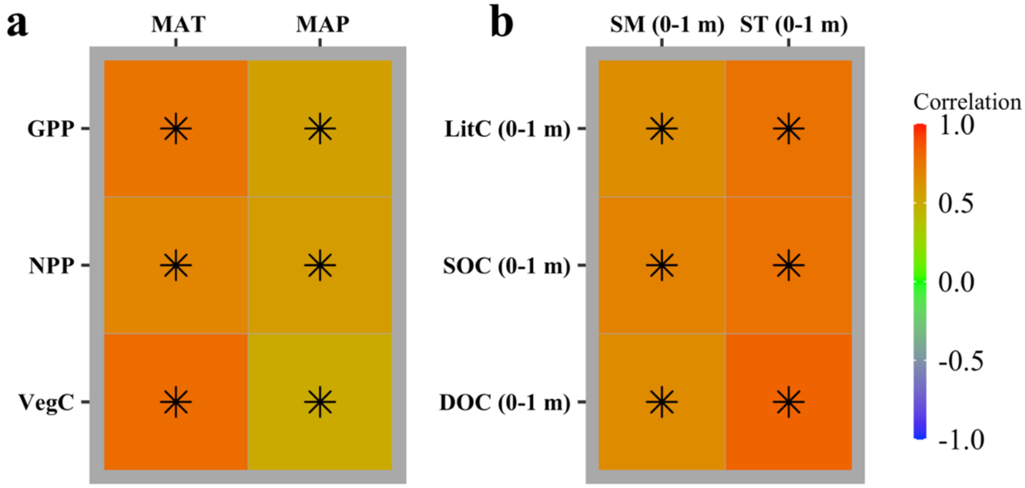

Fig. S13. Heatmap showing Pearson's correlation between the CLM-Microbe model simulated (a) GPP, NPP, and VegC and MAT and MAP and (b) HR, SR, FBC in the top 1 m, BBC in the top 1 1 m, DOC in the top 1 m, SOC in the top 1 m, and LitC in the top 1 m and SM and ST in the top 1 m from 1901 to 2016. GPP: gross primary productivity; NPP: net primary productivity; HR: heterotrophic respiration; SR: soil respiration; DOC: dissolved organic carbon; SOC: soil organic carbon; FBC: fungal biomass carbon; BBC: bacterial biomass carbon; VegC: vegetation carbon; LitC: litter carbon; MAT: mean annual temperature; MAP: mean annual precipitation; ST: soil temperature; SM: soil moisture. Black asterisks indicate significant correlations (P<0.05).

The area-weighted average of GPP, NPP, and VegC were significantly correlated with those of MAT and MAP (P<0.05; Figure S13a). However, the correlations with MAT are stronger than with MAP. At the grid level, MAP and MAT had widely significant correlations with GPP, NPP, and VegC. The spatial patterns of those correlations were similar among GPP, NPP, and VegC, but different between MAT and MAP (Figure S14). The MAT mostly showed significant positive correlations with GPP, NPP, and VegC (P<0.05; Figure S14a, S14c, and S14e). But we also found significant negative correlations of MAT with GPP, NPP, and VegC in southeast North America, South Asia, southern Africa, and central and northern Australia/Oceania (P<0.05). Despite the similar spatial patterns among GPP, NPP, and VegC in correlations with MAT and MAP, there were differences in the strengths and signs of their correlations. For example, both GPP and VegC had significant positive correlations with MAT in northeast South America (P<0.05), while correlations between NPP and MAT were weak negative in such regions. Both GPP and NPP showed significant positive correlations with MAT in central Africa (P<0.05), while the correlation between VegC and MAT was weak in that area (P>0.05). Significant positive correlations of GPP, NPP, and VegC with MAP were also widely found (P<0.05; Figure S14b, S14d, and S14f). However, we also found weak negative correlations in the northern and east edge of Asia and central Africa. In addition, although correlations of MAP with GPP, NPP, and VegC were similar in spatial patterns, correlations with GPP and NPP tended to be stronger than with VegC.

The area-weighted average of DOC, SOC, and LitC in the top 1 m were significantly correlated with that of ST and SM in the top 1 m (P<0.05; Figure S13b). However, the strengths of correlations depended on both environmental controls, with correlations of DOC, SOC, and LitC in the top 1 m with ST (0-1 m) being stronger than with SM (0-1 m). While correlations DOC, SOC, and LitC in the top 1 m were in similar strength with ST (0-1 m) or SM (0-1 m).

In contrast, soil and litter variables were more widely and positively correlated with ST than with SM in the top 1 m (Figure S15). The DOC and SOC in the top 1 m displayed similar spatial patterns (Figure S15a & S15c). We found significant and positive correlations of DOC and SOC with ST in the top 1 m in most grids across the globe (P<0.05). However, we also found some girds with negative correlations in central North America, Europe, Asia, South America, Africa, and Australia/Oceania. In contrast, correlations between LitC and ST in the top 1 m were equally found to be positive and negative (Figure S15e). Significant positive correlations were observed in central Europe and Asia, northeast South America, central and east coast of Africa, and southern and central Australia/Oceania, while significant negative correlations were distributed in northeast Asia (P<0.05). Correlations of DOC and SOC with SM in the top 1 m were similar in spatial patterns, with significant and positive correlations widely observed (P<0.05; Figure S15b & S15d). But we also observed negative correlations at middle and low latitudes in North America, Europe, and Asia, east coast of South America and Africa, and southern Australia/Oceania. In contrast, correlations between LitC and SM in the top 1 m were mostly negative and significant (P<0.05; Figure S15f). In addition, some grids with significant and positive correlation coefficients were scattered throughout central Africa, southwest Asia, and central and northern Australia/Oceania (P<0.05).

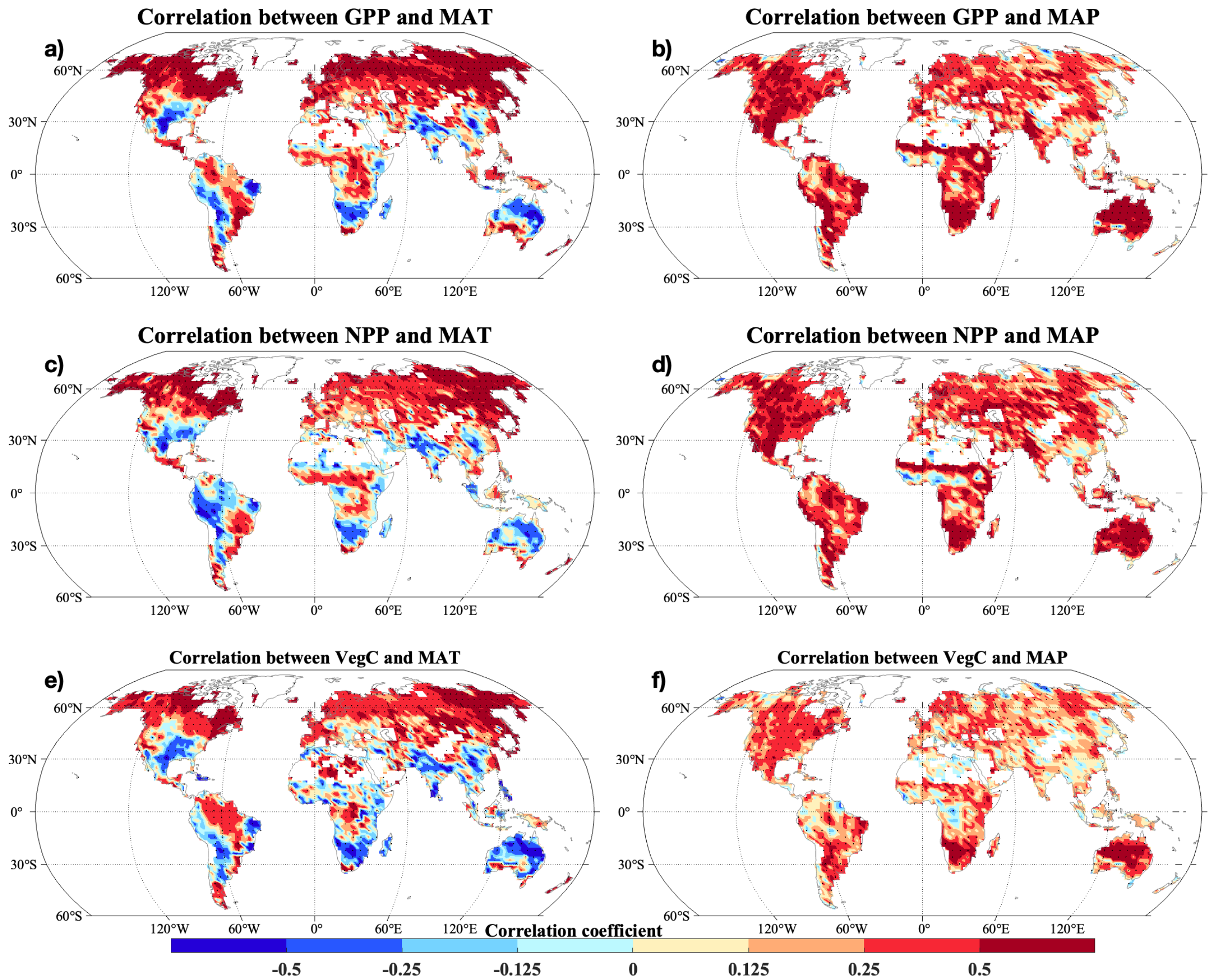

Fig. S14. Pearson's correlation between the CLM-Microbe model simulated (a-b) GPP, (c-d) NPP, and (e-f) VegC and (a, c, and e) MAT and (b, d, and f) MAP from 1901 to 2016. GPP: gross primary productivity; NPP: net primary productivity; VegC: vegetation carbon; MAT: mean annual temperature; MAP: mean annual precipitation. Black dot in each grid indicates significant correlation (P<0.05).

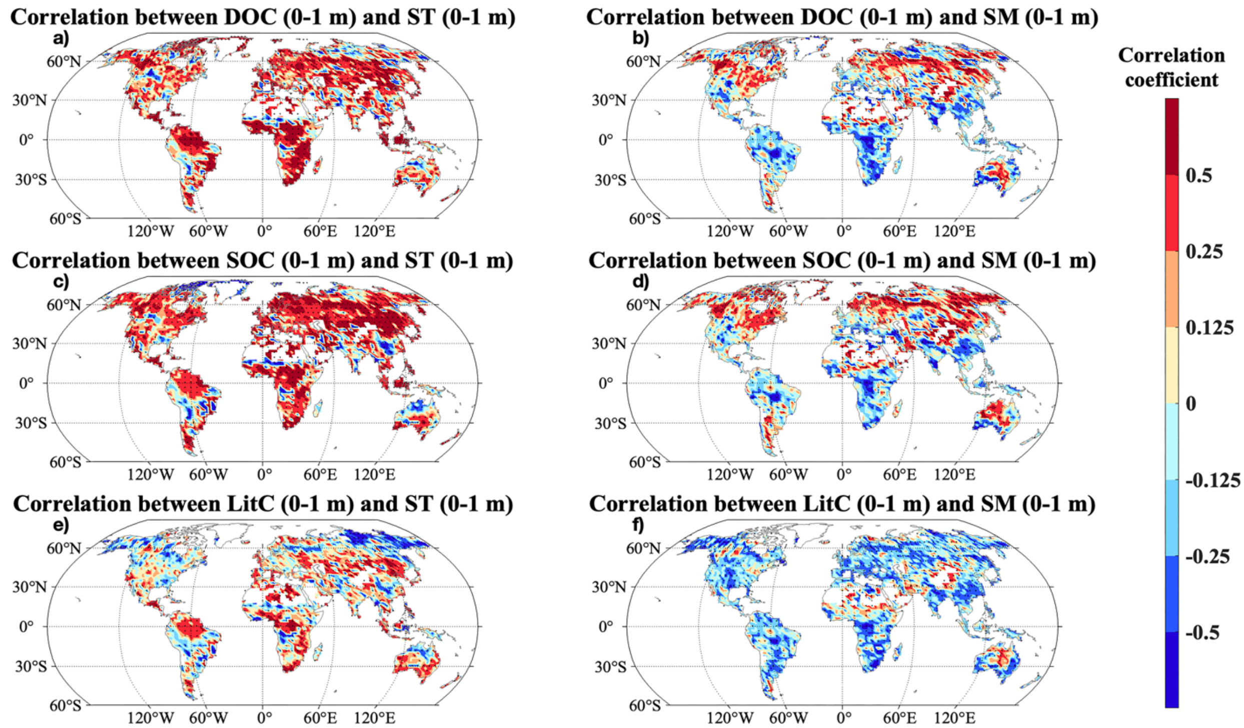

Fig. S15. Pearson's correlation between the CLM-Microbe model simulated (a-b) DOC in the top 1 m, (c-d) SOC in the top 1 m, and (e-f) LitC and (a, c, and e) ST and (b, d, and f) SM in the top 1 m from 1901 to 2016. DOC: dissolved organic carbon; SOC: soil organic carbon; LitC: litter carbon; ST: soil temperature; SM: soil moisture. Black dot in each grid indicates significant correlation (*P*<0.05)

References

Ågren, A. M., Haei, M., Blomkvist, P., Nilsson, M. B., and Laudon, H.: Soil frost enhances stream dissolved organic carbon concentrations during episodic spring snow melt from boreal mires, Global Change Biology, 18, 1895-1903, 2012.

Andreasson, F., Bergkvist, B., and Bååth, E.: Bioavailability of DOC in leachates, soil matrix solutions and soil water extracts from beech forest floors, Soil Biology and Biochemistry, 41, 1652-1658, 2009.

Camino-Serrano, M., Guenet, B., Luyssaert, S., Ciais, P., Bastrikov, V., De Vos, B., Gielen, B., Gleixner, G., Jornet-Puig, A., and Kaiser, K.: ORCHIDEE-SOM: modeling soil organic carbon (SOC) and dissolved organic carbon (DOC) dynamics along vertical soil profiles in Europe, Geoscientific Model Development, 11, 937-957, 2018.

Cherrier, J., Bauer, J., and Druffel, E.: Utilization and turnover of labile dissolved organic matter by bacterial heterotrophs in eastern North Pacific surface waters, Marine Ecology Progress Series, 139, 267-279, 10.3354/meps139267, 1996.

Cookson, W. R., Osman, M., Marschner, P., Abaye, D. A., Clark, I., Murphy, D. V., Stockdale, E. A., and Watson, C. A.: Controls on soil nitrogen cycling and microbial community composition across land use and incubation temperature, Soil Biology and Biochemistry, 39, 744-756, 2007.

Don, A. and Schulze, E.-D.: Controls on fluxes and export of dissolved organic carbon in grasslands with contrasting soil types, Biogeochemistry, 91, 117-131, 2008.

Fang, H., Cheng, S., Wang, Y., Yu, G., Xu, M., Dang, X., Li, L., and Wang, L.: Changes in soil heterotrophic respiration, carbon availability, and microbial function in seven forests along a climate gradient, Ecological Research, 29, 1077-1086, 2014a.

Fang, H., Cheng, S., Yu, G., Xu, M., Wang, Y., Li, L., Dang, X., Wang, L., and Li, Y.: Experimental nitrogen deposition alters the quantity and quality of soil dissolved organic carbon in an alpine meadow on the Qinghai-Tibetan Plateau, Applied Soil Ecology, 81, 1-11, 2014b.

Fao: Global Soil Organic Carbon Map (GSOCmap) : Technical Report, FAO, Rome, Italy, 167 pp.2018.

Fröberg, M., Jardine, P. M., Hanson, P. J., Swanston, C. W., Todd, D. E., Tarver, J. R., and Garten, C. T.: Low dissolved organic carbon input from fresh litter to deep mineral soils, Soil Science Society of America Journal, 71, 347-354, 2007.

Fujii, K., Hartono, A., Funakawa, S., Uemura, M., and Kosaki, T.: Fluxes of dissolved organic carbon in three tropical secondary forests developed on serpentine and mudstone, Geoderma, 163, 119-126, 2011.

Fujii, K., Uemura, M., Hayakawa, C., Funakawa, S., Kosaki, T., and Ohta, S.: Fluxes of dissolved organic carbon in two tropical forest ecosystems of East Kalimantan, Indonesia, Geoderma, 152, 127-136, 2009.

Funakawa, S., Hirai, H., and Kyuma, K.: Soil-forming processes under natural forest north of Kyoto in relation to soil solution composition, Soil Science and Plant Nutrition, 38, 101-112, 1992.

Ghani, A., Dexter, M., Carran, R. A., and Theobald, P. W.: Dissolved organic nitrogen and carbon in pastoral soils: the New Zealand experience, European Journal of Soil Science, 58, 832-843, 2007.

Gommers, P. J. F., Schie, B. J. v., Dijken, J. P. v., and Kuenen, J. G.: Biochemical limits to microbial growth yields: An analysis of mixed substrate utilization, Biotechnology and Bioengineering, 32, 86-94, 10.1002/bit.260320112, 1988.

Guo, Z., Wang, Y., Wan, Z., Zuo, Y., He, L., Li, D., Yuan, F., Wang, N., Liu, J., and Song, Y.: Soil dissolved organic carbon in terrestrial ecosystems: Global budget, spatial distribution and controls, Global Ecology and Biogeography, 2020.

He, L., Lipson, D. A., Rodrigues, J. L. M., Mayes, M., Björk, R. G., Glaser, B., Thornton, P., and Xu, X.: Dynamics of Fungal and Bacterial Biomass Carbon in Natural Ecosystems: Site-level Applications of the CLM-Microbe Model, Journal of Advances in Modeling Earth Systems, 13, e2020MS002283, https://doi.org/10.1029/2020MS002283, 2021.

He, L., Rodrigues, J. L. M., Soudzilovskaia, N. A., Barceló, M., Olsson, P. a. A., Song, C., Tedersoo, L., Yuan, F., Yuan, F., and Lipson, D. A.: Global biogeography of fungal and bacterial biomass carbon in topsoil, Soil Biology and Biochemistry, 108024, 2020.

Jones, D. L., Hughes, L. T., Murphy, D. V., and Healey, J. R.: Dissolved organic carbon and nitrogen dynamics in temperate coniferous forest plantations, European journal of soil science, 59, 1038-1048, 2008.

Kawahigashi, M., Sumida, H., and Yamamoto, K.: Seasonal changes in organic compounds in soil solutions obtained from volcanic ash soils under different land uses, Geoderma, 113, 381-396, 2003.

Kirchman, D. L., Suzuki, Y., Garside, C., and Ducklow, H. W.: High turnover rates of dissolved organic carbon during a spring phytoplankton bloom, Nature, 352, 612-614, 10.1038/352612a0, 1991.

Li, W., Yang, G., Chen, H., Tian, J., Zhang, Y., and Peng, C.: Soil available nitrogen, dissolved organic carbon and microbial biomass content along altitudinal gradient of the eastern slope of Gongga Mountain, Acta Ecologica Sinica, 33, 266-271, 2013.

Liu, C. P. and Sheu, B. H.: Dissolved organic carbon in precipitation, throughfall, stemflow, soil solution, and stream water at the Guandaushi subtropical forest in Taiwan, Forest Ecology and Management, 172, 315-325, 2003.

Liu, S., Hu, R., Cai, G., Lin, S., Zhao, J., and Li, Y.: The role of UV-B radiation and precipitation on straw decomposition and topsoil C turnover, Soil Biology and Biochemistry, 77, 197-202, 2014.

Liu, T., Liu, C., Zhang, W., and Tu, C.: Concentrations and migration features of dissolved organic carbon in the soils of slope lands in Karst area, China Environmental Science, 29, 248-253, 2009.

Lu, Y., Wassmann, R., Neue, H.-U., and Huang, C.: Dynamics of dissolved organic carbon and methane emissions in a flooded rice soil, Soil Science Society of America Journal, 64, 2011-2017, 2000.

Macdonald, A. J., Murphy, D. V., Mahieu, N., and Fillery, I. R. P.: Labile soil organic matter pools under a mixed grass/lucerne pasture and adjacent native bush in Western Australia, Soil Research, 45, 333-343, 2007.

Marques, J. D. d. O., Luizão, F. J., Teixeira, W. G., and Ferreira, S. J. F.: Variations of dissolved organic carbon and soil physical properties under different land uses in Central Amazônia, Volume 36, Número 2, Pags. 611-622, 2012.

Maxin, C. R. and Kögel-Knabner, I.: Partitioning of polycyclic aromatic hydrocarbons (PAH) to water-soluble soil organic matter, European Journal of Soil Science, 46, 193-204, 1995.

McDowell, W. H. and Wood, T.: Podzolization: soil processes control dissolved organic carbon concentrations in stream water, Soil Science, 137, 23-32, 1984.

Montano, N. M., Sandoval-Pérez, A. L., García-Oliva, F., Larsen, J., and Gavito, M. E.: Microbial activity in contrasting conditions of soil C and N availability in a tropical dry forest, Journal of tropical ecology, 25, 401-413, 2009.

Moore, J. C., McCann, K., and de Ruiter, P. C.: Modeling trophic pathways, nutrient cycling, and dynamic stability in soils, Pedobiologia, 49, 499-510, 2005.

Neff, J. C. and Hooper, D. U.: Vegetation and climate controls on potential CO2, DOC and DON production in northern latitude soils, Global Change Biology, 8, 872-884, 2002.

Panneer Selvam, B., Laudon, H., Guillemette, F., and Berggren, M.: Influence of soil frost on the character and degradability of dissolved organic carbon in boreal forest soils, Journal of Geophysical Research: Biogeosciences, 121, 829-840, 2016.

Pesántez, J., Mosquera, G. M., Crespo, P., Breuer, L., and Windhorst, D.: Effect of land cover and hydro-meteorological controls on soil water DOC concentrations in a high-elevation tropical environment, Hydrological Processes, 32, 2624-2635, 2018.

Rousk, J. and Bååth, E.: Fungal biomass production and turnover in soil estimated using the acetate-in-ergosterol technique, Soil Biology and Biochemistry, 39, 2173-2177, 10.1016/j.soilbio.2007.03.023, 2007.

Rousk, J. and Bååth, E.: Growth of saprotrophic fungi and bacteria in soil, FEMS Microbiology Ecology, 78, 17-30, 2011.

Schippers, A., Neretin, L. N., Kallmeyer, J., Ferdelman, T. G., Cragg, B. A., John Parkes, R., and Jørgensen, B. B.: Prokaryotic cells of the deep sub-seafloor biosphere identified as living bacteria, Nature, 433, 861-864, 10.1038/nature03302, 2005.

Schwendenmann, L. and Veldkamp, E.: The role of dissolved organic carbon, dissolved organic nitrogen, and dissolved inorganic nitrogen in a tropical wet forest ecosystem, Ecosystems, 8, 339-351, 2005.

Senga, Y., Hiroki, M., Nakamura, Y., Watarai, Y., Watanabe, Y., and Nohara, S.: Vertical profiles of DIN, DOC, and microbial activities in the wetland soil of Kushiro Mire, northeastern Japan, Limnology, 12, 17-23, 2011.

Shao, X., Yang, W., and Wu, M.: Seasonal dynamics of soil labile organic carbon and enzyme activities in relation to vegetation types in Hangzhou Bay tidal flat wetland, PLoS One, 10, e0142677, 2015.

Sinsabaugh, R. L., Manzoni, S., Moorhead, D. L., and Richter, A.: Carbon use efficiency of microbial communities: stoichiometry, methodology and modelling, Ecology Letters, 16, 930-939, 2013.

Sinsabaugh, R. L., Turner, B. L., Talbot, J. M., Waring, B. G., Powers, J. S., Kuske, C. R., Moorhead, D. L., and Shah, J. J. F.: Stoichiometry of microbial carbon use efficiency in soils, Ecological Monographs, 86, 172-189, 10.1890/15-2110.1, 2016.

Spears, J. D., Holub, S. M., Harmon, M. E., and Lajtha, K.: The influence of decomposing logs on soil biology and nutrient cycling in an old-growth mixed coniferous forest in Oregon, USA, Canadian Journal of Forest Research, 33, 2193-2201, 2003.

Strickland, M. S. and Rousk, J.: Considering fungal: bacterial dominance in soils–methods, controls, and ecosystem implications, Soil Biology and Biochemistry, 42, 1385-1395, 2010.

Thornton, P. E. and Rosenbloom, N. A.: Ecosystem model spin-up: Estimating steady state conditions in a coupled terrestrial carbon and nitrogen cycle model, Ecological Modelling, 189, 25-48, 2005.

Viovy, N.: CRUNCEP Version 7 - Atmospheric Forcing Data for the Community Land Model, Research Data Archive at the National Center for Atmospheric Research, Computational and Information Systems Laboratory [dataset], 10.5065/PZ8F-F017, 2018.

Waldrop, M. P., Wickland, K. P., White Iii, R., Berhe, A. A., Harden, J. W., and Romanovsky, V. E.: Molecular investigations into a globally important carbon pool: Permafrost-protected carbon in Alaskan soils, Global change biology, 16, 2543-2554, 2010.

Wallander, H. a., Göransson, H., and Rosengren, U.: Production, standing biomass and natural abundance of 15 N and 13 C in ectomycorrhizal mycelia collected at different soil depths in two forest types, Oecologia, 139, 89-97, 2004.

Wang, Y.-L., Yang, C.-M., Zou, L.-M., and Cui, H.-Z.: Spatial distribution and fluorescence properties of soil dissolved organic carbon across a riparian buffer wetland in Chongming Island, China, Pedosphere, 25, 220-229, 2015.

Warner, D. L., Bond-Lamberty, B. P., Jian, J., Stell, E., and Vargas, R.: Global Gridded 1-km Annual Soil Respiration and Uncertainty Derived from SRDB V3, 10.3334/ORNLDAAC/1736, 2019.

Weintraub, M. N. and Schimel, J. P.: The seasonal dynamics of amino acids and other nutrients in Alaskan Arctic tundra soils, Biogeochemistry, 73, 359-380, 2005.

Wheeler, P. A., Gosselin, M., Sherr, E., Thibaultc, D., Kirchman, D. L., Benner, R., and Whitledge, T. E.: Active cycling of organic carbon in the central Arctic Ocean, Nature, 380, 697-699, 10.1038/380697a0, 1996.

Wieder, W.: Regridded Harmonized World Soil Database v1.2, 10.3334/ORNLDAAC/1247, 2014.

Wu, H., Song, X., Zhao, X., Peng, X., Zhou, H., Hallett, P. D., Hodson, M. E., and Zhang, G.-L.: Accumulation of nitrate and dissolved organic nitrogen at depth in a red soil Critical Zone, Geoderma, 337, 1175-1185, 2019.

Xi, M., Zi, Y., Wang, Q., Wang, S., Cui, G., and Kong, F.: Assessment of the content, structure, and source of soil dissolved organic matter in the coastal wetlands of Jiaozhou Bay, China, Physics and Chemistry of the Earth, Parts A/b/c, 103, 35-44, 2018.

Xu, X., Thornton, P. E., and Post, W. M.: A global analysis of soil microbial biomass carbon, nitrogen and phosphorus in terrestrial ecosystems, Global Ecology and Biogeography, 22, 737-749, 2013.

Yao, S., Qin, J., Peng, X., and Zhang, B.: The effects of vegetation on restoration of physical stability of a severely degraded soil in China, Ecological Engineering, 35, 723-734, 2009.

Ying, C., Shaoqiang, W., Jingyuan, W., Peichl, M., and Falahatar, S.: Dissolved organic carbon dynamics and controls of planted slash pine forest soil in subtropical region in southern China, Journal of Resources and Ecology, 4, 105-114, 2013.

Zeh, L., Limpens, J., Erhagen, B., Bragazza, L., and Kalbitz, K.: Plant functional types and temperature control carbon input via roots in peatland soils, Plant and Soil, 438, 19-38, 2019.

Zhao, M., Heinsch, F. A., Nemani, R. R., and Running, S. W.: Improvements of the MODIS terrestrial gross and net primary production global data set, Remote Sensing of Environment, 95, 164-176, 10.1016/j.rse.2004.12.011, 2005.

Zhong, X.-l., Li, J.-t., Li, X.-j., Ye, Y.-c., Liu, S.-s., Hallett, P. D., Ogden, M. R., and Naveed, M.: Physical protection by soil aggregates stabilizes soil organic carbon under simulated N deposition in a subtropical forest of China, Geoderma, 285, 323-332, 2017.

Zhou, W.-j., Sha, L.-q., Zhang, Y.-p., Song, Q.-h., Liu, Y.-t., Deng, Y., and Deng, X.-b.: Characteristics and influencing factors of soil dissolved organic carbon and nitrogen in a tropical seasonal rainforest in Xishuangbanna, Southwest China, China.Journal of Beijing Forestry University, 38, 34-41, 2016.